strained optimum geometry would remain an optimum geometry even if the symmetry constraints were removed.

Registry No. 1, 157-20-0; **2**, 157-18-6; **3**, 157-17-5; thiirene-d_2, 65923-97-9; thiirene-*2,3*-$^{13}C_2$, 84057-45-4; thiirene-d_1, 63965-75-3; thiirene-*2*-$^{13}C_1$, 63965-74-2; oxirene-d_2, 84057-46-5; oxirene-*2,3*-$^{13}C_2$, 84057-47-6; oxirene-d_1, 84057-48-7; oxirene-*2*-$^{13}C_1$, 84057-49-8; 1-*H*-azirine-*1*-d_1, 84057-50-1; 1-*H*-azirine-*2,3*-d_2, 84057-51-2; azirine-d_3, 84057-52-3; 1-*H*-azirine-*2,3*-$^{13}C_2$, 84064-67-5; 1-*H*-azirine-*2*-d_1, 84057-53-4; 1-*H*-azirine-*1,2*-d_2, 84057-54-5; 1-*H*-azirine-*2*-$^{13}C_1$, 84057-55-6.

Location of Cupric Ions in X Zeolites by Electron Spin Echo Spectrometry: Contrast between Sodium and Potassium X Zeolites

Tsuneki Ichikawa[†] **and Larry Kevan***

Contribution from the Faculty of Engineering, Hokkaido University, Sapporo, 060, Japan, and Department of Chemistry, University of Houston, Houston, Texas 77004.

Received April 22, 1982

Abstract: Electron spin echo spectra have been measured for X zeolite containing a small amount of Cu^{2+}. Locations of the Cu^{2+} and the structure of adsorbed molecules have been determined by analyzing the observed nuclear modulation effects on the electron spin echo spectra. In hydrated sodium X zeolite Cu^{2+} is located in hexagonal prisms connecting two sodalite units (site SI), where they are fully coordinated to six lattice oxygens. Upon dehydration at 673 K, the Cu^{2+} environment changes slightly as shown by resolved hyperfine splittings in the $g_\perp$ region and a shorter Cu^{2+}–aluminum distance. Cu^{2+} is still thought to be in site I but may be displaced somewhat toward the sodalite cage. In hydrated potassium X zeolite Cu^{2+} is in sites on a line perpendicular to hexagonal windows between the sodalite and super cages and displaced into the super cages (site SII*). Each Cu^{2+} in site SII* is coordinated to three lattice oxygens in the hexagonal window and three water molecules in the super cage. Upon partial dehydration of the potassium X zeolite at 373 K in air, part of the Cu^{2+} migrate into a site in the center of the hexagonal windows (site II), where each Cu^{2+} is coordinated to three lattice oxygens and two water molecules, one in a sodalite cage and the other in a super cage. In dehydrated potassium X zeolite Cu^{2+} moves to the same site as in dehydrated sodium X zeolite. The difference in the site locations in *hydrated* sodium and potassium X zeolites is explained in terms of the different hydration energies of alkali cations.

Introduction

The cation locations in zeolite catalysts have been extensively studied because of their influence on catalytic properties. When the cations are paramagnetic, electron spin resonance (ESR) spectroscopy has been widely used to gain information about the location and coordination environment of the cations.[1] Cupric ion has been widely studied because this d^9 ion has an easily observed ESR spectrum which is rather sensitive to the Cu^{2+} environment.[2,3] However, the ESR spectrum does not give direct information about the local structure of the cations, such as the distance and number of first solvation shell nuclei. When the cations are surrounded by magnetic nuclei, this information is directly included in the superhyperfine interaction between the electron spins and the nuclear spins, but this is generally too weak for detection by normal ESR.

We have recently demonstrated that electron spin echo (ESE) spectroscopy is useful for selectively detecting the weak superhyperfine interaction between surrounding magnetic nuclei and paramagnetic species on catalytic oxides.[4-12] This superhyperfine interaction shows up as a modulation of the decay of the time domain ESE spectrum. By proper analysis of this modulation one can determine types, number, and distances of magnetic nulcei surrounding the paramagnetic species.[13]

In the present work ESE spectrometry is used to elucidate the local structure of trace Cu^{2+} in hydrated and dehydrated zeolite X with sodium and potassium as exchangeable cations. It is shown that the site location is critically dependent on the nature of the major cation.

Experimental Section

Binder-free Linde 13X (Na–X) was used as a starting material. Potassium X zeolite (K–X) was prepared by conventional exchange of Na^+ in Na–X with K^+. Partially Cu^{2} exchanged Na–X and K–X (CuNa–X and CuK–X, respectively) were prepared by ion exchanging as described previously.[4] The extent of exchange of Na^+ or K^+ by Cu^{2+} was approximately 0.3%. After filtration the excess amount of water was taken out by pressing the wet samples between filter paper. The resulting samples are designated as hydrated. Deuterated counterparts of the hydrated samples were prepared by exchanging all the H_2O with D_2O (Stohler Isotope Chemicals) at ambient temperature. Completely dehydrated samples were prepared by evacuating the hydrated samples at ambient temperature for 1 h, heating up to 673 K at increasing temperature for intervals of 1 h in vacuo, oxidizing at 673 K for 2 h under an oxygen pressure of 760 torr, and then evacuating for 15 h at 673 K. Methanol (Merck, spectroscopic grade) and its deuterated counterparts (Stohler Isotope Chemicals) were used as received. These compounds were adsorbed by exposing the dehydrated samples to the vapor at room temperature.

ESR spectra were obtained at 77 K on a Varian E-4 spectrometer. ESE spectra were obtained at 4.2 K on a home-built spectrometer with 1-kW maximum microwave power and typical pulse widths of 20 ns.[14] The nuclear modulations from Al in the zeolite framework were detected by measuring the two-pulse ESE spectra of the zeolite containing no

---

[†] Hokkaido University.

* Author to whom inquiries should be addressed at University of Houston.

(1) Lunsford, J. H. *Adv. Catal.* **1976**, *26*, 137.
(2) Conesa, J. C.; Soria, J. *J. Chem. Soc., Faraday Trans. 1* **1979**, *75*, 406.
(3) Herman, R. G.; Flentge, D. R. *J. Phys. Chem.* **1978**, *82*, 720.
(4) Ichikawa, T.; Kevan, L. *J. Chem. Soc., Faraday Trans. 1* **1981**, *77*, 2567.
(5) Ichikawa, T.; Kevan, L. *J. Am. Chem. Soc.* **1981**, *103*, 5355.
(6) Narayana, M.; Li, A. S. W.; Kevan, L. *J. Phys. Chem.* **1981**, *85*, 132.
(7) Ichikawa, T.; Yoshida, H.; Kevan, L. *J. Chem. Phys.* **1981**, *75*, 2485.
(8) Ichikawa, T.; Yoshida, H.; Kevan, L. *J. Phys. Chem.* **1982**, *86*, 881.
(9) Ichikawa, T.; Kevan, L. *J. Am. Chem. Soc.* **1980**, *102*, 2650.
(10) Narayana, M.; Kevan, L. *J. Am. Chem. Soc.* **1981**, *103*, 5729.
(11) Narayana, M.; Kevan, L. *J. Chem. Phys.* **1981**, *75*, 3269.
(12) Narayana, M.; Kevan, L. *J. Chem. Phys.* **1982**, *76*, 3999.
(13) Kevan, L. In "Time Domain Electron Spin Resonance"; Kevan, L.; Schwartz, R. N.; Eds.; Wiley-Interscience: New York, 1979; Chapter 8.
(14) Ichikawa, T.; Kevan, L.; Narayana, P. A. *J. Phys. Chem.* **1979**, *83*, 3378.

0002-7863/83/1505-0402$01.50/0

deuterated compounds. The nuclear modulations from deuterium in the deuterated adsorbates were detected by measuring three-pulse ESE spectra with 0.26 μs selected between the first and second microwave pulses to detect the deuterium modulation while suppressing the aluminum modulation.[13]

Analysis

The theory of the nuclear modulation has been described in detail[13,15,16] so the method of data analysis is only briefly described. The deuterium modulations were analyzed by the least-squares method. The experimental ESE spectrum was compared with the theoretical one by

$$\text{ERROR} = \frac{1}{N}\sum_{i=1}^{N}[V^{\text{ex}}(T_i) - D(T_i)\{V^{\text{th}}(T_i,r,a)\}^n]^2 \qquad (1)$$

where $V^{\text{ex}}(T_i)$ is the observed intensity of the ESE signal, T_i is the time interval between the second and the third microwave pulses, $D(T_i)$ is an unknown monotonic decay function, $V^{\text{th}}(T_i,r,a)$ is the theoretical intensity of the ESE signal for *one* magnetic nucleus with an electron spin–nuclear spin distance of r and an isotropic hyperfine coupling constant of a, and n is the number of equivalent nuclei surrounding the electron spin. A generalized exponential function is used as the decay function

$$D(T_i) = \exp(a_0 + a_1T_i + a_2T_i^2) \qquad (2)$$

where the parameters, a_0, a_1, and a_2 are suitably selected. Equation 1 is written as

$$\text{ERROR} = \frac{1}{N}\sum_{i=1}^{N}\{V^{\text{ex}}(T_i)\}^2\left[1 - \exp(a_0 + a_1T_i + a_2T_i^2)\frac{\{V^{\text{th}}(T_\text{i},r,a)\}^n}{V^{\text{ex}}(T_i)}\right]^2 \qquad (3a)$$

The term $\exp(a_0 + a_1T_1 + a_2T_2^2)[V^{\text{th}}(T_i,r,a)]^n/V^{\text{ex}}(T_i)$ is unity for any T_i if the simulated ESE signal is exactly the same as the experimental one. Therefore, the value of this term should be *close* to unity for acceptable simulations. We therefore approximate eq 3a by using the relation

$$\lim_{x\to1}(1 - x) = \lim_{x\to1}(\ln x)$$

to obtain

$$\text{ERROR} \simeq \frac{1}{N}\sum_{i=1}^{N}[V^{\text{ex}}(T_i)]^2[a_0 + a_1T_1 + a_2T_2^2 + n\ln[V^{\text{th}}(T_\text{i},r,a)] - \ln[V^{\text{ex}}(T_i)]]^2 \qquad (3b)$$

The parameters a_0, a_1, a_2 are determined for given r, a, and n by the equations

$$\frac{\partial}{\partial a_0}\text{ERROR} = 0,\ \frac{\partial}{\partial a_1}\text{ERROR} = 0,\ \frac{\partial}{\partial a_2}\text{ERROR} = 0 \qquad (4)$$

The best set of parameters, r, n, a, satisfy the equations

$$\frac{\partial}{\partial r}\text{ERROR} = 0,\ \frac{\partial}{\partial a}\text{ERROR} = 0,\ \frac{\partial}{\partial n}\text{ERROR} = 0 \qquad (5)$$

The values of n are constrained to be integral and can be determined to the nearest integral n up to $n \sim 8$; r is determined to ±0.01 nm, a to ±10%.

The Al modulations were qualitatively analyzed by a ratio analysis method.[14] In this method two smooth curves joining all the maxima and minima of the Al modulation are drawn. These curves measured as a function of the time interval between the first and second pulses, τ, are denoted by $V_{\max}(\tau)$ and $V_{\min}(\tau)$, respectively. The experimental modulation amplitude is defined by

$$R^{\text{ex}}(\tau) = \frac{V_{\max}(\tau)}{V_{\min}(\tau)} \qquad (6)$$

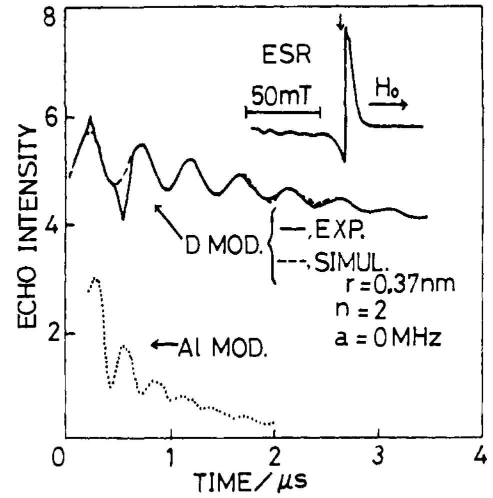

Figure 1. ESR and ESE spectra for hydrated CuNa–X at 4 K. The arrow on the ESR spectrum indicates the magnetic field for the ESE measurements. The three-pulse ESE spectrum showing deuterium modulation (D mod) was obtained with CuNa–X hydrated by D_2O. The two-pulse ESE spectrum showing aluminum modulation (Al Mod) was obtained with CuNa–X hydrated by H_2O.

When an electron spin is surrounded by n equivalent nuclear spins, the theoretical modulation amplitude is given by

$$R^{\text{th}}{}_{\text{T}}(\tau) = \{R^{\text{th}}(\tau,r,a)\}^n \qquad (7)$$

By equating $R^{\text{ex}}(\tau)$ to $R^{\text{th}}{}_{\text{T}}(\tau)$ and taking the log twice we have

$$\log\{\log R^{\text{ex}}(\tau)\} - \log\{\log R^{\text{th}}(\tau,r,a)\} = \log n \qquad (8)$$

Therefore, if we compare two ESE modulations with different n and the same r and a, the difference of the double logarithmic modulation amplitudes gives a τ-independent constant which is equilavent to the logarithmic ratio of the number of surrounding nuclei,

$$\log\{\log R_1^{\text{ex}}(\tau)\} - \log\{\log R_2^{\text{ex}}(\tau)\} = \log(n_2/n_1) \qquad (9)$$

Results

Figure 1 shows the ESR, three-pulse ESE, and two-pulse ESE spectra for hydrated CuNa–X. The ESR spectrum with $g_\parallel > g_\perp$ can be assigned as Cu^{2+} under distorted octahedral symmetry.[17] The best simulation of the three-pulse deuterium modulation indicates that the Cu^{2+} is surrounded by two deuterons (one water molecule) with a Cu^{2+}–$D(D_2O)$ distance of 0.37 nm. When water is directly coordinated to Cu^{2+} this distance is typically 0.26 nm[4,5] so it is evident that the Cu^{2+} is not directly coordinated to the water molecule. The two-pulse ESE spectrum shows deep Al modulation, indicating that the Cu^{2+} is surrounded by several aluminums.

The deuterium modulation is not observed after evacuating the hydrated CuNa–X at 323 K for 20 h. Figure 2 shows the ESR and two-pulse ESE spectra obtained after this treatment. This mild dehydration results in the development of sharply defined Cu^{2+} hyperfine splittings in the $g_\perp$ region of the ESR spectrum. The aluminum modulation is a little deeper than in the hydrated CuNa–X. Strong dehydration at 673 K for 15 h gives the aluminum modulation shown in Figure 3. A prominent double-frequency component is observed, indicating that the aluminums are yet closer to Cu^{2+} or that Cu^{2+} has migrated to a new site. Rehydrated CuNa–X exhibits the same ESR and ESE spectra as those for the originally hydrated CuNa–X.

Adsorption of methanol on strongly dehydrated CuNa–X does not change the aluminum modulation from that in Figure 3. However, weak deuterium modulation can be seen for specifically deuterated methanols. Analysis of this deuterium modulation gives a Cu^{2+}–$D(CD_3OH)$ distance of 0.40 nm with $n = 3$ and a Cu^{2+}–$D(CH_3OD)$ distance of 0.46 nm with $n = 1$. The solvation

---

(15) Mims, W. B.; Peisach, J.; Davis, J. *J. Chem. Phys.* **1977**, *66*, 5536.

(16) Ichikawa, T.; Kevan, L.; Bowman, M. K.; Dikanov, S. A.; Tsvetkov, D. *J. Chem. Phys.* **1979**, *71*, 1167.

(17) Hathaway, B. J.; Billing, D. E. *Coord. Chem. Rev.* **1970**, *5*, 143.

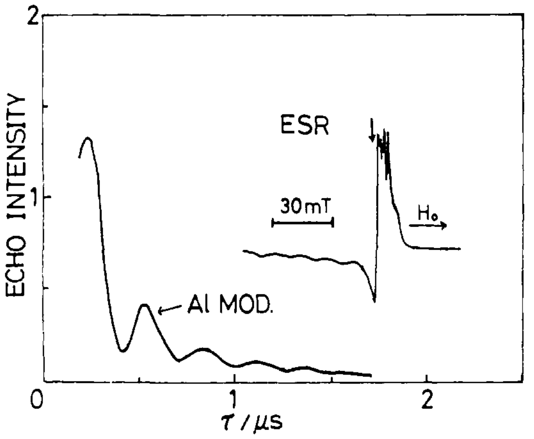

Figure 2. ESR and two-pulse ESE spectra for CuNa-X dehydrated at 323 K for 20 h under vacuum. An arrow on the ESR spectrum indicates the magnetic field for the ESE measurement.

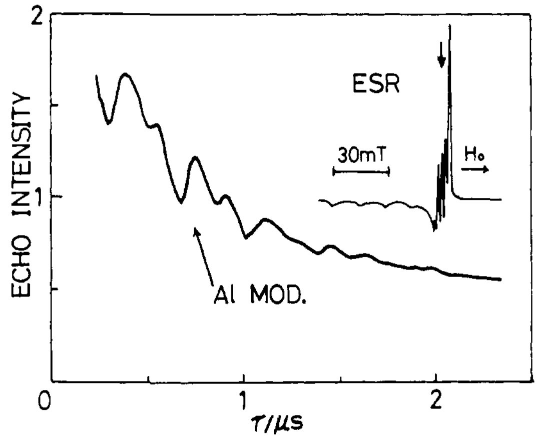

Figure 3. ESR and two-pulse ESE spectrum for CuNa-X dehydrated at 673 K for 15 h under vacuum. An arrow on the ESR spectrum indicates the magnetic field for the ESE measurement. Similar spectra are seen for CuK-X.

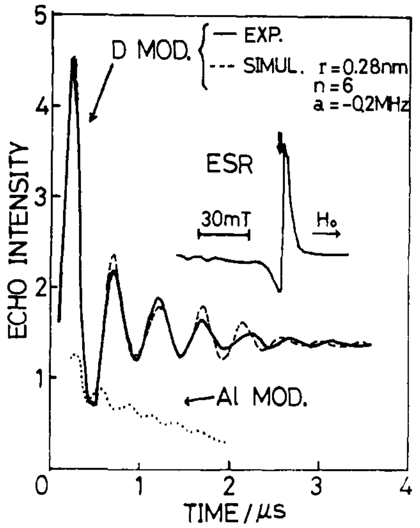

Figure 4. ESR and ESE spectra for hydrated CuK-X at 4 K. The arrow on the ESR spectrum indicates the magnetic field for the ESE measurements. The three-pulse ESE spectrum showing deuterium modulation was obtained with CuK-X hydrated by D_2O. The two-pulse ESE spectrum showing aluminum modulation was obtained with CuK-X hydrated by H_2O.

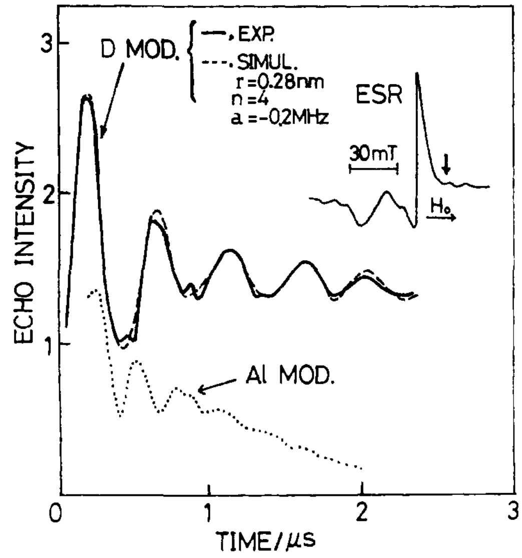

Figure 5. ESR and ESE spectra for CuK-X heated at 373 K for 10 h in air. The arrow on the ESR spectrum shows the magnetic field for the ESE measurements. The three-pulse ESE spectrum showing deuterium modulation was obtained from CuK-X originally hydrated with D_2O. The two-pulse ESE spectrum showing aluminum modulation was obtained from CuK-X originally hydrated with H_2O.

of Cu^{2+} in frozen methanol solutions gives corresponding distances of 0.37 and 0.26 nm.[18] These shorter distances indicate that methanol is not directly coordinated to Cu^{2+} in CuNa-X.

The ESR and ESE spectra for hydrated Cu-X are shown in Figure 4. Although the ESR spectra are similar, the deuterium modulation is much deeper than that for hydrated CuNa-X. The best simulation of the deuterium modulation shows that the Cu^{2+} is directly coordinated to three water molecules with a Cu^{2+}-D-(D_2O) distance of 0.28 nm. The aluminum modulation is shallower than that of hydrated CuNa-X. Evacuation of the hydrated CuK-X at 323 K does not cause any significant change in the ESR and ESE spectra in contrast to CuNa-X.

As shown in Figure 5, partial dehydration of CuK-X at 373 K in air causes the development of a new ESR spectrum with $g_\perp > g_\parallel$. The ESE spectra corresponding to this new ESR spectrum show deeper aluminum modulation and shallower deuterium modulation than those for hydrated CuK-X. The best simulation of the deuterium modulation indicates that the Cu^{2+} is coordinated to two water molecules with a Cu^{2+}-D(D_2O) distance of 0.28 nm. The original ESR spectrum with $g_\parallel > g_\perp$ is not completely converted to the new one even after heating for 20 h at 373 K. Heating of CuK-X at 373 K under vacuum does not give the new ESR spectrum with $g_\perp > g_\parallel$ but shows the same *ESR* and ESE spectra as those for completely dehydrated CuK-X discussed below.

The ESR and ESE spectra for strongly dehydrated CuK-X heated at 673 K for 15 h are similar to those for strongly dehydrated CuNa-X. Rehydrated CuK-X gives the same ESR and ESE spectra as those for originally hydrated CuK-X.

Adsorption of methanol on strongly dehydrated CuK-X does not change the aluminum modulation. Weak deuterium modulation is seen for specifically deuterated methanols. Analysis of this deuterium modulation gives a Cu^{2+}-D(CD_3OH) distance of 0.39 nm with $n = 3$ and a Cu^{2+}-D(CH_3OD) distance of 0.41 nm with $n = 1$. These long distances again indicate no direct coordination of the methanol to the Cu^{2+}.

Figure 6 compares the amplitude of the aluminum modulations. The difference of the double logarithmic modulation amplitude between hydrated CuNa-X and hydrated CuK-X gives an almost time-independent constant of 0.3, which means that the Cu^{2+}-Al distance and *a* are the same for both the samples, but that the number of surrounding Al in hydrated CuK-X is one-half of that in hydrated CuNa-X. The rapid decrease of the aluminum modulation amplitude for the Cu^{2+} with $g_\perp > g_\parallel$ in CuK-X suggests that the Cu-Al distance is shorter than that in hydrated CuK-X.

---

[18] Ichikawa, T.; Kevan, L. *J. Phys. Chem.* **1980**, *84*, 1955.

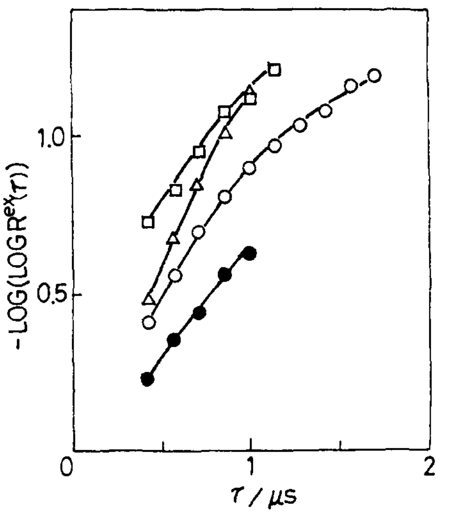

Figure 6. Comparison of the amplitude of the aluminum modulation for hydrated CuNa-X (○). CuNa-X dehydrated at 323 K for 20 h under vacuum (●), hydrated CuK-X (□), and the Cu^{2+} with $g_\perp > g_\parallel$ in CuK-X dried at 373 K for 10 h (△).

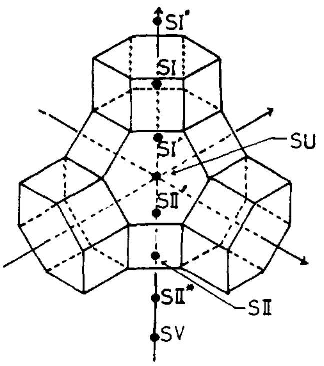

Figure 7. Cation sites and their designations in X zeolite.

Discussion

Zeolite X is composed of AlO_2 and SiO_2 with an Al/(Al + Si) ratio of 0.45 bonded together to form truncated cuboctahedra with eight hexagonal windows and six square windows. These cubooctahedra are called sodalite cages and are tetrahedrally bonded tobether by hexagonal prisms to form larger super cages. Figure 7 shows various cation sites identified by X-ray crystallography.[19] SU is near the center of the sodalite cage, SV is near the center of the super cage, SI is the center of the hexagonal prism, SII is the center of the hexagonal window between the sodalite cage and the super cage, and SII' and SII* correspond to displacement into the sodalite cage and into the super cage, respectively, along an axis perpenicular to a hexagonal window. Finally SIII is used in a broad sense to cover sites in the super cage near the square windows.

Since no water molecule is directly coordinated to the Cu^{2+} in hydrated CuNa-X and since it shows strong aluminum modulation, one can assign that Cu^{2+} to SI where it is fully coordinated to six lattice oxygens with distorted octahedral symmetry. This site is shown in Figure 8. In SI the Cu^{2+} is sandwiched by two hexagonal windows, so that the average number of nearest aluminums is $12 \times 0.45 = 5.4$. The disappearance of deuterium modulation from water on heating hydrated CuNa-X under vacuum at 323 K indicates that water is easily desorbed under these conditions and hence only weakly adsorbed in the zeolite framework. This dehydration seems to cause a slight contraction of the hexagonal prism as evidenced by an increase in the aluminum modulation depth. Upon complete dehydration at 673 K the ESR spectrum changes significantly, and the average Cu^{2+}–Al distance decreases so that a double modulation pattern characteristic of shorter interaction distances becomes apparent. This could be due to a contraction of the hexagonal prism or a movement of Cu^{2+} toward the sodalite cage to site SI'. Previous studies have suggested that Cu^{2+} in dehydrated X and Y zeolites are in sites SI and SI'.[24] Upon rehydration water enters the sodalite cages and interacts to expand the hexagonal prism or to return Cu^{2+} to its original site in the hydrated zeolite. However, this interaction does not occur when methanol is adsorbed because methanol is too large to enter the sodalite cages.

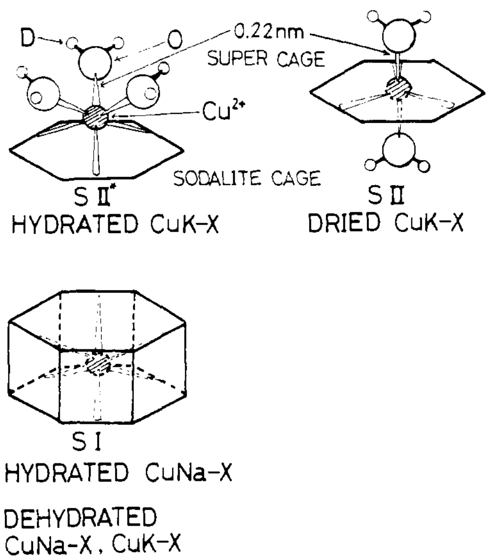

Figure 8. Models for Cu^{2+} site locations in X zeolite.

In hydrated CuK-X the Cu^{2+} is assigned to SII* in the super cage where it is octahedrally coordinated to three lattice oxygens in a hexagonal window between the sodalite cage and the super cage and to three water molecules in the super cage (see Figure 8). Since the aluminum modulation indicates that the Cu^{2+}–Al distance is approximately the same in SII* as in SI, it suggests that the Cu^{2+} in SII* is displaced from the hexagonal window into the super cage by about half the height of a hexagonal prism which is about ~0.15 nm. In SII* the number of nearest aluminums is 2.7 in a hexagonal window which is half the number in SI. This is supported by the qualitative analysis of the aluminum modulation in Figure 6. We caution, however, that the analysis of the aluminum modulation may be complicated by contributions from sodium modulation.

Contrary to the uncoordinated water molecules in hydrated CuNa-X, the coordinated water molecules in hydrated CuK-X cannot be detached by evacuation at 323 K. Part of the coordinated water molecules in hydrated CuK-X are detached by heating the sample up more, to 373 K. Since the water molecules in the sodalite cage are more difficult to desorb than those in the super cage, the Cu^{2+} with fewer coordinated water molecules in the super cage migrates into SII in a hexagonal window and coordinates with one additional water molecule in the sodalite cage (see Figure 8). In SII the Cu^{2+} is trigonal bipyramidally coordinated to three lattice oxygens in the hexagonal window and to two water molecules, one in the super cage and the other in the sodalite cage. The unpaired electron of the Cu^{2+} under trigonal-bipyramidal coordination has a d_{z^2} ground state, which gives an ESR spectrum with $g_\perp > g_\parallel$.[20] The Cu^{2+}–Al distance is slightly shorter in SII than in SII* so the partially dehydrated CuK-X shows slightly deeper aluminum modulation with a faster modulation decay.

Upon complete dehydration of CuK-X, the Cu^{2+} migrates into the same site as that for completely dehydrated CuNa-X. Upon rehydration the water molecules penetrate into the sodalite cage and Cu^{2+} moves back to SII*.

---

[19] Smith, J. V. In "Zeolite Chemistry and Catalysis"; Rabo, J. A., Ed.; American Chemical Society: Washington, D.C., 1976; Chapter 1.

[20] Herman, R. G. *Inorg. Chem.* **1979**, *18*, 995.

The difference in the Cu^{2+} site location between hydrated CuNa–X and hydrated CuK–X can be attributed to the difference in the hydration energies of Na^+ and K^+. The hydration energy for Na^+ is greater than that of K^+ because of the difference in their ionic radii which are 0.097 and 0.133 nm, respectively. Let us assume that the Cu^{2+} is initially located in SII*. The migration of Cu^{2+} from the SII* to SI requires the displacement of an alkali cation from SI.[21,22] Since the hexagonal prism offers the same electrostatic field to both Na^+ and K^+, the energy for removing an unhydrated alkali cation is the same for Na^+ and K^+. However, the net energy gain for transferring an unhydrated alkali cation from SI to a more exposed site, where it will be hydrated, is greater for Na^+ because it has a larger hydration energy. So it is energetically more favorable for Cu^{2+} to displace Na^+ from SI than to displace K^+. This argument seems consistent with our findings that a small concentration of Cu^{2+} in hydrated CuNa–X migrates into the SI sites whereas Cu^{2+} stays in SII* in hydrated CuK–X. After dehydration the hydration energy argument is moot and the Cu^{2+} location is the same in CuK–X and CuNa–X.

It is relevant to compare our structural results with previous literature based only on ESR and optical spectra.[23] In most cases a critical comparison of CuNa–X and CuK–X was not carried out. However, this was the focus of a recent optical study.[23] In hydrated CuNa–X the optical spectra have been assigned to $Cu^{2+}(H_2O)_6$ species in the super cages. We have found that the $Cu^{2+}(H_2O)_6$ species can be removed by repeated washing of an A zeolite with water and the same may apply to X and Y zeolites. So the $Cu^{2+}(H_2O)_6$ species may be simply entrapped solution and may not be a cation state or site of catalytic relevance.

The optical spectrum for Cu^{2+} in CuK–X has been found to be different from that for $Cu^{2+}(H_2O)_6$ in CuNa–X and has been assigned to hydrated Cu^{2+} in the sodalite cages.[23] This assignment is admittedly speculative and we suggest that it should be reassigned to SII* in the super cage. Distinct changes in the optical spectra occur on dehydration and a band grows in at higher wavenumber; we suggest that this new band should be assigned to the site in or near the hexagonal prism that we deduce from ESE studies.

It is interesting that this optical study points out the differences between Cu^{2+} locations in hydrated CuK–X and CuNa–X. However, we believe that the specific site locations suggested from that study need to be modified based on the ESE studies which are able to count numbers of coordinated waters.

Acknowledgment. This research was supported by the National Science Foundation and the Robert A. Welch Foundation. We especially thank Dr. M. Narayana for his incisive critical comments.

Registry No. Cu, 7440-50-8; methanol, 67-56-1.

---

(21) Mortier, W. J.; Bosmans, H. J. *J. Phys. Chem.* **1971**, *75*, 3327.

(22) Mortier, W. J.; Bosmans, H. J.; Uytterhoeven, J. B. *J. Phys. Chem.* **1972**, *76*, 650.

(23) deWilde, W.; Schoonhoydt, R. A.; Uytterhoeven, J. B. *ACS Symp. Ser.* **1977**, No. 40, 132–143.

(24) Conesa, J. C.; Soria, J. *J. Chem. Soc., Faraday Trans. 1* **1978**, *74*, 406.

Coordination Shifts in ^{15}N Nuclear Magnetic Resonance Spectra of Glycinato and Ethylenediamine Ligands in Cobalt(III) Complexes

N. Juranić*[†] and R. L. Lichter*

Contribution from the City University of New York, Department of Chemistry, Hunter College, New York, New York 10021. *Received February 1, 1982*

Abstract: Nitrogen-15 nuclear magnetic resonance spectra of the 12 complexes of the type $[Co(ox)_x(gly)_y(en)_z]$ have been determined (oxH_2 = oxalic acid, glyH = glycine, en = ethylenediamine). ^{15}N resonances of glycinato and ethylenediamine ligands exhibit shielding coordination shifts ranging from −19 to −62 ppm. Coordination shifts are very sensitive to the trans influence; a nitrogen nucleus in an amino group trans to oxygen is shielded by about 18 ppm more than one in a group trans to nitrogen. The cis influence is about 4 times less pronounced and in the opposite direction. An estimation of the Cornwell–Santry effect in low-spin d^6 complexes suggests that this may be the major cause of the observed coordination shifts as well as of coordination shift variations arising from trans and cis influences.

Introduction

Shielding of nuclei directly bonded to transition-metal ions with spin-paired d^6 electronic configurations has been observed in a number of complexes.[1-4] These shifts are sensitive both to the nature of the ligands and to the geometrical configuration of the complexes.[3,5-7] Hence, nuclear magnetic resonance (NMR) spectroscopy of nuclei directly bonded to metal ions could show promise as a sensitive probe for bonding and for coordination geometry. However, few experimental data are available, so that systematic investigation is still required in order to establish areas and limits of applicability of this technique. ^{15}N NMR spectroscopy is of particular interest because nitrogen is the ligating atom of many ligands that are important in coordination chemistry and biochemistry.

The only published systematic study of cobalt(III) complexes by ^{15}N NMR spectroscopy is on the effect of ligand replacement in pentaamminecobalt(III) complexes.[6] ^{15}N chemical shifts vary widely with the nature of X in $[CoX(^{15}NH_3)_5]^{n+}$. Futhermore, chemical shifts of the NH_3 group depend on the trans or cis geometry with respect to X. These changes have been shown to be much larger than could be accounted for by paramagnetic

---

[†] Visiting Fulbright scholar (1980–1981), University of Belgrade, Department of Chemistry and Physical Chemistry, 11001 Beograd, Yugoslavia.

(1) Bremley, R.; Figgis, B. N.; Nyholm, R. S. *J. Chem. Soc. A* **1967**, *861*–863.

(2) Matwiyoff, N. A.; Asprey, L. B.; Wageman, W. F.; Reisfeld, H. J.; Fukushima, E. *Inorg. Chem.* **1969**, *8*, 750–753.

(3) Fung, B. M.; Wei, S. C. *J. Magn. Reson.* **1970**, *3*, 1–4.

(4) Bose, K. S.; Abbott, E. H. *Inorg. Chem.* **1977**, *16*, 3190–3194.

(5) Lehman, J. W.; Fung, B. M. *Inorg. Chem.* **1970**, *8*, 1197–1200.

(6) Nakashima, Y.; Muto, M.; Tagaki, J.; Kawana, K. *Chem. Lett.* **1975**, 1075–1080.

(7) Ozaki, Y.; Kyogoku, Y. *J. Chem. Soc., Chem. Commun.* **1979**, *76*–77.

0002-7863/83/1505-0406$01.50/0